

# Non-equilibrium Plasmons in a Quantum Wire Single Electron Transistor

Jaek U. Kim, Ilya V. Krive,\* and Jari M. Kinaret

Department of Applied Physics, Chalmers University of Technology and Göteborg University, SE-412 96 Gothenburg, Sweden

(Dated: February 7, 2020)

We analyze a single electron transistor composed of two semi-infinite one dimensional quantum wires and a relatively short segment between them. We describe each wire section by a Luttinger model, and treat tunneling events in the sequential approximation when the system's dynamics can be described by a master equation. We show that the steady state occupation probabilities in the strongly interacting regime depend only on the energies of the states and follow a universal form that depends on the source-drain voltage and the interaction strength.

PACS numbers: 71.10.Pm, 73.23.Hk, 73.63.-b

Strongly interacting one dimensional (1D) electron systems that can be described by Tomonaga-Luttinger (TL) model [1] are under great interest due to recent experimental observations especially in the systems of single-walled carbon nanotubes (SWNT) [2, 3, 4, 5]. The Luttinger Liquid (LL), which is generalization of the TL model, is characterized by the absence of fermionic quasi-particles; instead, the elementary excitations take the form of bosonic charge and spin density waves [6].

Motivated by recent experiment by Postma *et al.* [7], we theoretically investigate a 1D single electron transistor (SET). Schematic description of the system is that a finite wire segment, later called a quantum dot, is weakly coupled to two long wires as depicted in Fig. 1. Two point-like impurities or other defects in a long nanotube may result in equivalent physics. We model the system as a finite LL segment and two semi-infinite LL leads. The leads are connected to electron reservoirs which keep them in internal equilibria. The chemical potentials of the leads are controlled by source-drain voltage ( $V_{sd}$ ), and we assume that tunneling barriers between leads and dot are high enough that sequential tunneling is the dominant charge transport mechanism. Closely related studies based on a different set of approximations were recently published by Braggio and co-workers [8, 9]. If the tunneling barriers are lower, or if sequential tunneling is blocked (Coulomb blockade), correlations between tunneling events across the left and right junctions become important. Transport in this regime has been discussed by Thorwart *et al.* [10].

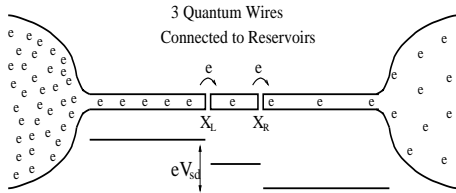


FIG. 1: Model system. Two long wires are adiabatically connected to reservoirs and a short wire is connected to the two by weak coupling.

In this Letter, we analyze the steady-state occupation probabilities of the many-body states on the dot. We will show that in the strongly interacting regime they are characterized by a *universal* distribution that depends on the applied voltage and the interaction strength. Next, we calculate the current-voltage curves for the characteristic parameters of a metallic SWNT.

Carbon nanotubes have four transport channels including spin degeneracy [3, 4]. The electron transport through quantum wires (QWs) is determined mostly by charge effects so it is reasonable to consider, as a first approximation [5], the contribution of the total charge sector to SET characteristics, and postpone the discussion of the role of the other channels to a later date. The effective Hamiltonian  $\hat{H} = \hat{H}_0 + \hat{H}_T$  for this branch is

$$\begin{aligned} \hat{H}_0 &= \sum_{l=(L,D,R)} \frac{\pi \hbar v_F}{g L_l} \sum_{m=1}^{\infty} m \hat{b}_{l,m}^\dagger \hat{b}_{l,m} + \frac{\pi \hbar v_F}{2g^2 L_D} (\hat{N} - N_G)^2, \\ \hat{H}_T &= \sum_{\lambda=(L,R)} \sum_{a=(i,\sigma)} \left[ t_\lambda \hat{\psi}_{D,a}^\dagger(X_\lambda) \hat{\psi}_{\lambda,a}(X_\lambda) + H.C. \right]. \end{aligned} \quad (1)$$

Here  $\hat{H}_0$  is the bosonized LL Hamiltonian and the tunneling Hamiltonian  $\hat{H}_T$  describes *bare electrons* tunneling through barriers at the points  $X_L$  and  $X_R$ , where indices  $i=1,2$  and  $\sigma=\pm$  identify bare electrons. The parameter  $g$  indicates interaction strength,  $g=1$  for non-interacting electrons and  $g \rightarrow 0$  for strong repulsive interaction. The term  $\hat{E}_C = \frac{\pi \hbar v_F}{2g^2 L_D} (\hat{N} - N_G)^2$  is on-dot zero-mode contribution including the Coulomb charging energy, where  $N_G$  is a dimensionless gate voltage control parameter in the range  $N_G \in [0,1]$  (integer values correspond to maximum blockade and half-integer to off-blockade). Leads are assumed to be semi-infinite with continuous spectra; the dot, in contrast, has finite size  $L_D$  and discrete energy spectrum with the plasmon level spacing  $\Delta E = \pi \hbar v_F / g L_D$ .

We describe the system's dynamics using a master equation within a sequential tunneling regime where un-

\*Also at B.I. Verkin Institute for Low Temperature Physics and Engineering, Lenin ave., 47, Kharkov 61103, Ukraine

correlated single electron hoppings are dominant transport mechanism [11, 12],

$$\begin{aligned} & (\partial/\partial t)P(N, \{n\}) \\ &= \sum_{N'=N\pm 1} \sum_{\{n'\}} [P(N', \{n'\})\Gamma(N', \{n'\} \rightarrow N, \{n\}) \\ & \quad - P(N, \{n\})\Gamma(N, \{n\} \rightarrow N', \{n'\})], \end{aligned} \quad (2)$$

where the variables  $(N, \{n\})$  represent a state of the dot with  $N$  excess electrons and a set of the occupation numbers  $\{n\} = (n_1, n_2, \dots, n_m, \dots)$  of the plasmon states with momenta  $p_m = m \cdot \pi\hbar/L_D$ ,  $P$  are the occupation probabilities of the dot-states  $(N, \{n\})$ , and  $\Gamma = \Gamma_L + \Gamma_R$  are the transition rates due to tunneling through junctions at  $X_L$  and  $X_R$ . The lead degrees of freedom were integrated out since the leads are locally in equilibria.

If the transition rates are known, it is straightforward to determine steady-state occupation probabilities by solving master equation (2) for  $(\partial/\partial t)P(N, \{n\}) = 0$  with the constraint  $\sum_{N, \{n\}} P(N, \{n\}) = 1$ .

The transition rates  $\Gamma_{L/R}$  are evaluated within the golden rule approximation with respect to the tunneling Hamiltonian  $\hat{H}_T$  using the standard bosonization technique [6]. As a function of the states on the dot and their energies the rates are given by

$$\begin{aligned} & \Gamma_{L/R}(N, \{n\} \rightarrow N', \{n'\}) = 8\pi|t_{L/R}|^2/\hbar \\ & \times \gamma(E_D(N', \{n'\}) - E_D(N, \{n\}) \mp (N' - N)eV_{L/R}) \\ & \times |\langle N', \{n'\} | \psi_D^\dagger \delta_{N', N+1} + \psi_D \delta_{N', N-1} | N, \{n\} \rangle|^2, \end{aligned} \quad (3)$$

where “-/+” sign corresponds to index “L/R” and the voltage drops across junctions are  $V_{L/R} = \frac{R_{L/R}}{(R_L + R_R)} V_{sd}$  for the tunneling resistances  $R_{L/R} \propto |t_{L/R}|^{-2}$  when dc source drain voltage  $V_{sd}$  is supplied. Lead contributions are given by a spectral function  $\gamma(\epsilon)$  [9, 11]

$$\begin{aligned} \gamma(\epsilon) &= \frac{1}{2\pi\hbar} \int_{-\infty}^{\infty} dt e^{i\epsilon t} \langle \Psi_{\lambda, a}(X_\lambda, 0) \Psi_{\lambda, a}^\dagger(X_\lambda, t) \rangle \\ &= \frac{1}{2\pi\hbar} \frac{1}{\pi v_F} \left( \frac{2\pi\Lambda_g}{\hbar v_F \beta} \right)^\alpha \left| \Gamma\left(\frac{\alpha+1}{2} + i\frac{\beta\epsilon}{2\pi}\right) \right|^2 \frac{e^{-\beta\epsilon/2}}{\Gamma(\alpha+1)} \end{aligned} \quad (4)$$

Here  $\alpha = (g^{-1} - 1)/4$ , appropriate for an end-contacted four-channel wire such as SWNT [4],  $\beta = 1/k_B T$  is the inverse temperature in the leads, and  $\Lambda_g = \Lambda g^{1/(1-g)}$  where  $\Lambda$  is a short wavelength cut-off. At zero temperature,  $\gamma(\epsilon)$  is proportional to a power of energy,  $\lim_{T \rightarrow 0} \gamma(\epsilon) \propto \Theta(-\epsilon)|\epsilon|^\alpha$ . The dot energy  $E_D$  is obtained by solving the eigenvalue problem of the Hamiltonian (1), and is given by a sum of the zero mode energy  $E_C(N) = (\pi\hbar v_F/2g^2 L_D) \cdot (N - N_G)^2$  and the plasmonic excitation energy  $E_B(\{n\}) = (\pi\hbar v_F/gL_D) \cdot \sum_m m \cdot n_m$ ,

$$E_D(N, \{n\}) = \frac{\pi\hbar v_F}{L_D} \left[ \frac{(N - N_G)^2}{2g^2} + \sum_{m=1}^{\infty} \frac{m \cdot n_m}{g} \right] \quad (5)$$

The zero-mode overlap is unity for  $N' = N \pm 1$  and vanishes otherwise, and the overlaps of the plasmonic states

can be written in terms of Laguerre polynomials as [13]

$$\begin{aligned} & |\langle \{n'\} | \psi_D^\dagger | \{n\} \rangle|^2 = \frac{1}{L_D} \left( \frac{\pi\Lambda}{L_D} \right)^\alpha \times \\ & \prod_{m=1}^{\infty} \left( \frac{1}{4mg} \right)^{|n'_m - n_m|} \frac{n_m^{(<)}}{n_m^{(>)}}! \left[ L_{n_m^{(<)}}^{|n'_m - n_m|} \left( \frac{1}{4mg} \right) \right]^2 \end{aligned} \quad (6)$$

where  $n_m^{(<)} = \min(n'_m, n_m)$  and  $n_m^{(>)} = \max(n'_m, n_m)$ . Notice that at low energies only the first few occupations  $n_m$  and  $n'_m$  in the product in Eq. (6) differ from zero, yielding non-unity factors to the transition rate.

With the analytically calculated transition rates (Eqs. (3)-(6)), we solve the master equation numerically and determine occupation probabilities of the many-body states. Hereafter we will present numerical results for the case with symmetric barriers, the dot size of  $L_D = 50n_m$  and the Fermi velocity of  $v_F = 8 \times 10^5 \text{ m/s}$  [5].

Fig. 2 shows (A) the occupation probabilities  $P(\{n\})$  versus the energies  $E_B(\{n\})$  of the many-body states of  $(N=0, \{n\})$  and (B) the averaged probabilities  $P(n) = \langle P(\{n\}) \rangle_n$  of degenerate states with energies  $E_B(n)$ . The degeneracy  $D(n)$  of  $E_B(n) = n \cdot \pi\hbar v_F/gL_D$  is the number of the many-body occupation configurations  $\{n\}$  that satisfy  $E_B(\{n\}) = E_B(n)$ , i.e.,  $\sum_m m \cdot n_m = n$ , which asymptotically follows the Hardy-Ramanujan formula [14]

$$D(n) \simeq e^{\pi\sqrt{2n/3}} / (4\sqrt{3}n). \quad (7)$$

As seen in Fig. 2(A), there is a dramatic change of the occupation probability distribution between a non-interacting ( $g=1$ ) and a strongly interacting ( $g \lesssim 0.24$ ) quantum dot. In the non-interacting case the occupation probabilities of degenerate many-body states vary widely as is natural since electrons tunnel independently of each other (apart from the Pauli principle); typically states with many long wavelength plasmons are more likely than states with few short wavelength excitations.

In contrast, in the strongly interaction regime all degenerate states are almost equally likely (variation of about 10% only, see the inset of Fig. 2(B)) and the occupation probability decreases nearly exponentially with its energy. The suppression of probability variations originates from interactions in the *central island* [16] and can be understood as a consequence of the separation of zero-modes and bosonic excitations in the strongly interacting limit even for a small system. The inclusion of spin effects in the central segment (spin is already included in the leads) introduces non-interacting degrees of freedom that results in increased fluctuations which can be suppressed by a magnetic field. In Fig. 2(B), we show that the average occupation probabilities  $P(n) = \langle P(\{n\}) \rangle_n$  decay nearly exponentially even in the weakly interacting regime,  $g \gtrsim 0.4$ , where the probabilities of degenerate states fluctuate strongly.

The nearly exponential decay of the average probabilities suggests a *Gibbs-like distribution*. However, there is no obvious reason why this non-equilibrium distribution should follow an equilibrium form. We obtain an

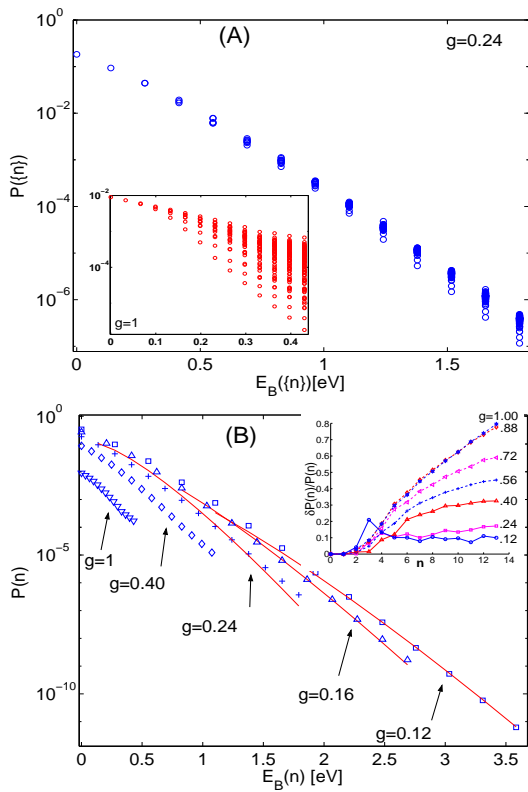


FIG. 2: (A) The occupation probabilities  $P(\{n\}) \equiv P(N=0, \{n\})$  as a function of the energies  $E_B(N=0, \{n\})$  of the many-body states on the dot for  $g = 0.24$  (SWNT) and for  $g = 1$  (non-interacting) in the inset. The degeneracy of the energy state  $E_B(n)$  is  $D(n) \simeq \exp(\pi\sqrt{2n/3})/(4\sqrt{3}n)$ , where  $n = \sum_m m \cdot n_m$  is the dimensionless energy (circles (o) represent individual many-body states). (B) Averaged probabilities  $P(n) = \langle P(\{n\}) \rangle_n$  as a function of the energy levels  $E_B(n)$ . Solid lines are analytic approximations  $P(n) \propto n^{-\frac{3}{2} \frac{\alpha+1}{n_{sd}} n}$  where  $n_{sd} = eV_{sd} \cdot (\pi\hbar v_F/gL_D)^{-1}$ . Inset shows the relative standard deviations of the probabilities,  $\langle \delta P(\{n\}) \rangle_n / P(n)$ , as a function of the dimensionless energy  $n = E_B(n) \cdot (\pi\hbar v_F/gL_D)^{-1}$  for  $g$ -values ranging from  $g = 1$  to  $g = 0.12$ . Implicit parameters are  $T = 50\text{mK}$ ,  $V_{sd} = g^{-1} \times 0.22\text{V}$ , and  $N_G = 0.5$ .

analytic approximation to  $P(n)$  at zero temperature by setting the on-dot transition elements in (6) to unity and considering the scattering-in and scattering-out processes for a particular many-body state  $\{n\}$ . In this approximation, all degenerate states have equal probabilities and the total scattering rates at a specific energy are given by the product of the lead contribution (4), which follows a power-law, and the degeneracy (7). The master equation now reads

$$\frac{\partial}{\partial t} P(n) = \sum_{n'} [P(n') D(n') \Gamma(n' \rightarrow n) - P(n) D(n) \Gamma(n \rightarrow n')] \quad (8)$$

where the total charge labels  $N$  have been suppressed. By solving the master equation using saddle point inte-

gral approximations, we obtain a differential equation for  $\ln[P(n)]$  and find that for a large  $E_B(n)$ ,  $P(n)$  is

$$P_{univ}(n) = Z^{-1} \cdot n^{-\frac{3}{2} \frac{\alpha+1}{n_{sd}} n} = Z^{-1} \cdot e^{-\frac{3}{2} \frac{\alpha+1}{n_{sd}} n \log n} \quad (9)$$

where  $n_{sd} = eV_{sd} \cdot (\pi\hbar v_F/gL_D)^{-1}$  is the dimensionless bias voltage and  $Z$  is the partition function. This distribution is *universal* in the sense that it does not depend on the precise form of the Hamiltonian of the dot as long as the excitation spectrum is bosonic and has linear dispersion. Over limited energy ranges, it resembles a *Gibbs distribution* with the effective temperature

$$k_B T_{eff}(n) \approx - \left( \frac{\partial \ln P(n)}{\partial E_n} \right)^{-1} = \frac{2}{3} \frac{eV_{sd}}{\alpha + 1} \frac{1}{1 + \log n} \quad (10)$$

In the range of our interest  $g \lesssim 0.24$  ( $g \simeq 0.24$  for a SWNT device [5]) and  $n \sim 10$ , this is approximately

$$k_B T_{eff} \simeq C(n) \cdot g \cdot eV_{sd}/2 \quad (11)$$

where  $1 \leq C(n) < 2$ .

As an application of the newly found distribution function, we investigate the current  $I(V)$  and the differential conductance  $G = dI/dV$  of the SWNT-SET with  $g = 0.24$ , as a function of gate voltage. Current  $I$  is easily calculated once the occupation probabilities  $P$  are known,

$$I = -e \sum_{N, \{n\}, \{n'\}} \left[ P(N, \{n\}) \Gamma_L(N, \{n\} \rightarrow N+1, \{n'\}) - P(N+1, \{n'\}) \Gamma_L(N+1, \{n'\} \rightarrow N, \{n\}) \right]. \quad (12)$$

Fig. 3 shows the  $I$ - $V$  characteristics: (A) off-Coulomb blockade with  $N_G = 0.5$  and (B) a blockade case with  $N_G = 0.35$  ( $I$  is in units proportional to  $|t_{L/R}|^2$ ).

At zero temperature, there are conductance peaks whenever voltage drop across a junction equals difference of two quantized energy levels,  $\Delta(eV) = E(N', n') - E(N, n)$ . At a finite temperature only peaks that overcome thermal broadening survive. For  $N_G = 0.5$  (Fig. 3(A)), electron numbers  $N=0$  and  $N=1$  have degenerate ground states which results in lifting of Coulomb blockade at zero bias voltage and yields equidistant conductance peaks separated by  $2\Delta E_B = 2(\pi\hbar v_F/gL_D)$ . In Fig. 3(B), there is no transport for low bias voltage due to Coulomb blockade gate voltage of  $N_G = 0.35$ . The main conductance peaks indicate transitions involving the ground state. The side peaks (a) in Fig. 3(A) and (a) to (c) in Fig. 3(B) are for transitions between excited states [9, 15]. The satellite peaks are smeared out at high temperature as shown in the  $T=77\text{K}$  plot because they result from transitions between excited states only.

Temperature broadens each transition, which smears conductance peaks or current kinks in the range  $|V - V_{peak}| \sim k_B T$  (compare  $T=50\text{mK}$  and  $T=77\text{K}$  in the figure). The inset in Fig. 3(A) shows conductance at zero bias voltage is proportional to a power of temperature,  $G_{V \rightarrow 0+}(T) \propto T^{\alpha^*}$ ,  $\alpha^* = \alpha - 1$  when  $k_B T < \Delta E_B$  and it

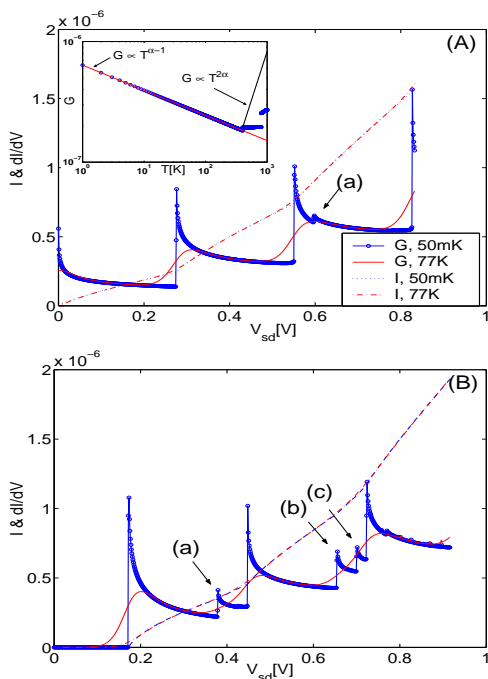


FIG. 3: Current  $I$  and differential conductance  $dI/dV$  as a function of source-drain voltage  $V_{sd}$  for  $g = 0.24$ . (A) Off-Coulomb blockade with  $N_G=0.5$  and (B) a Coulomb blockade with  $N_G=0.35$ , for which the conductance vanishes up to  $eV_{sd} = 0.3 \times \pi \hbar v_F / g^2 L_D$  at zero temperature.  $I$  is in units proportional to  $|t_{L/R}|^2$ . Inset in (A) shows power-law of conductance on temperature at zero bias voltage where solid line is  $G(T) = G(T_0) \cdot (T/T_0)^{\alpha-1}$  for  $k_B T < \Delta E_B$ . Implicit parameters are same as in Fig. 2.

is eventually expected to reach  $2\alpha$  when  $k_B T \gg \Delta E_B$  for which the dot displays continuous spectrum. It can be generalized to  $G_{V \rightarrow V_p^+}(T) \propto T^{\alpha-1}$  when  $k_B T < \Delta E_B$ .

The  $G$ - $V$  analyses agree with Braggio *et al.* [8, 9], noticing that our system has four channel renormalized exponent,  $\alpha = (g^{-1} - 1)/4$  and spin effects in the dot are not considered [17]. Since the results by Braggio *et al.* were obtained in a different approximation for the occupation probabilities, this comparison also shows that a simple  $I$ - $V$  measurement is rather insensitive to the on-dot distribution function (spin effects on the central dot are not expected to be sensitive either). However, the distribution function is expected to have a more pronounced impact on more sensitive probes such as noise measurements, which will be considered at elsewhere.

In conclusion, we have analyzed a quantum wire single electron transistor where each wire segment is described by a Tomonaga-Luttinger model. We have shown that in the sequential tunneling regime the steady-state occupation probabilities of the many-body states at the central dot follow a universal distribution that is determined by a competition between energy dependent tunneling rates and the degeneracy of the on-dot many-body quantum states. We have applied the non-equilibrium distribution to calculate the current-voltage characteristics of a SWNT-SET, and shown that the  $I$ - $V$  measurement is rather insensitive to the distribution function.

We acknowledge valuable discussions with R. I. Shekhter, L. Y. Gorelik and A. Kadigrobov, and the support of the Swedish Foundation for Strategic Research (QDNS and CARAMEL) and the Royal Swedish Academy of Sciences (KVA). I. Krive acknowledges the hospitality of Dept. of Applied Physics, Chalmers University of Technology and Göteborg University.

- 
- [1] S. Tomonaga, *Prog. Theor. Phys.* **5**, 544 (1950); J.M. Luttinger, *J. Math. Phys.* **4**, 1154 (1963).  
[2] S.J. Tans *et al.*, *Nature* **386**, 474 (1997).  
[3] R. Egger, and A.O. Gogolin, *Phys. Rev. Lett.* **79**, 5082 (1997).  
[4] C. Kane, L. Balents and M.P.A. Fisher, *Phys. Rev. Lett.* **79**, 5086 (1997).  
[5] M. Bockrath *et al.*, *Nature* **397**, 598 (1999); Z. Yao *et al.*, *Nature* **402**, 273 (1999).  
[6] For reviews, see V.J. Emery, *Highly Conducting One-Dimensional Solids*, edited by Devreese, Evrard and van Doren, 247 (Plenum press, 1979); F.D.M. Haldane, *J. Phys. C*, **14**, 2585 (1981); J. Voit, *Rep. Prog. Phys.* **58**, 977 (1995).  
[7] H.W.C. Postma *et al.*, *Science* **293**, 76 (2001).  
[8] A. Braggio *et al.*, *Europhys. Lett.* **50**, 236 (2000).  
[9] A. Braggio, M. Sasseti and B. Kramer, *Phys. Rev. Lett.* **87**, 146802 (2001).  
[10] M. Thorwart *et al.*, *Phys. Rev. Lett.* **89**, 196402 (2002);  
[11] A. Furusaki, *Phys. Rev. B* **57**, 7141 (1998).  
[12] A. Komnik and A.O. Gogolin, *cond-mat/0211474* (2002).  
[13] Identical expression for transitions in a magnetic field was derived by J. Schwinger, *Phys. Rev.* **91**, 728 (1953).  
[14] G.H. Hardy and S. Ramanujan, *Proc. London Math. Soc.* **17**, 75 (1918).  
[15] Note that, in Fig. 3(B), the peak corresponding to  $(N=0, n=j+1) \leftrightarrow (N=1, n=j)$  is missing at low  $T$  as it results from the transitions between (nearly degenerate) excited states.  
[16] A system with  $g_{lead}=g$  and  $g_{dot}=1$  shows that the averaged probabilities follow the analytic result (9) and the probability fluctuations for various  $g$ -values are almost identical to  $g_D=1$  case (inset of Fig. 2(A)). On the other hand, a system with  $g_{lead}=1$  and  $g_{dot}=g$  shows fluctuation suppressions as a function of  $g$ , similar to the inset of Fig. 2(B); however, the averaged probabilities follow Eq. (9) with  $\alpha=0$ . Finally, when the dot transition matrix elements in Eq. (6) are replaced by unity, it shows no fluctuation of the probabilities at all and averaged probabilities are in a good agreement with Eq. (9) for the whole range of interaction strength.  
[17] Including spin in the central segment results in additional peaks [9].